Ex vivo ^{1}H and ^{31}P magnetic resonance spectroscopy as a means for tumor characterization in ovarian cancer patients

YORAM ABRAMOV[1*], SHANI CARMI[2*], SHAOUL O. ANTEBY[3] and ISRAEL RINGEL[2]

[1]Department of Obstetrics and Gynecology, Carmel Medical Center, Technion University, Rappaport Faculty of Medicine, Haifa; Departments of [2]Pharmacology and [3]Obstetrics and Gynecology, Hadassah Hebrew University Medical School, Jerusalem, Israel

Received August 17, 2012; Accepted September 18, 2012

DOI: 10.3892/or.2012.2071

Abstract. We aimed to determine whether cells obtained from malignant ovarian tumors had different *ex vivo* ^{1}H- and ^{31}P (phosphorus-31)-magnetic resonance (MR) spectra compared to cells obtained from benign ovarian cysts. In addition, we aimed to assess the metabolic effects of chemotherapy on malignant cells obtained from peritoneal effusions of ovarian cancer patients. We included 20 ovarian cancer patients undergoing explorative laparotomy for tumor resection, 15 patients undergoing oophorectomy for benign ovarian cysts and 8 patients with advanced ovarian cancer with cancerous peritoneal effusion undergoing palliative percutaneous drainage. Ovarian and metastatic tissues were obtained from all patients undergoing laparotomy and analyzed using ^{1}H magnetic resonance spectroscopy (MRS). Cancerous cells from peritoneal effusions were incubated with 3 different anti-mitotic drugs (paclitaxel, cisplatin and carboplatin) at LC_{50} and the consequent metabolic changes were monitored using ^{31}P-MRS. ^{1}H-MRS revealed significantly higher intracellular lactate levels in cells obtained from ovarian tumors, most prominently in the moderately to poorly differentiated histological types, while total choline (Chol) compounds were higher in the moderately to poorly differentiated subgroup only. Ovarian cancer cells obtained from peritoneal effusions showed a significantly decreased glycerophosphocholine (GPC), glycerophosphoethanolamine (GPE) and uridine diphospho-sugar (UDPS) levels following *ex vivo* exposure to all 3 anti-mitotic drugs. *Ex vivo* ^{1}H-MRS identified significant metabolic differences between cells obtained from ovarian tumors compared to those originating in benign ovarian cysts, including increased lactate and total choline compound levels. The ^{31}P-MRS technique allowed characterization and monitoring of metabolic changes occurring in ovarian cancer cells in response to chemotherapy.

Correspondence to: Dr Yoram Abramov, Department of Obstetrics and Gynecology, Carmel Medical Center, Technion University, Rappaport Faculty of Medicine, Haifa, Israel
E-mail: yabramov@012.net.il

*Contributed equally

Abbreviations: ^{31}P, phosphorus-31; ADP, adenosine diphosphate; ATP, adenosine triphosphate; CEM, cells embedded in Matrigel; CGM, cells grown in monolayers; Chol, choline; GPC, glycerophosphocholine; GPE, glycerophosphoethanolamine; MHz, megaHertz; MR, magnetic resonance; MRS, magnetic resonance spectroscopy; NADP, nicotine adenine diphosphate; PBS, phosphate-buffered saline; PCr, phosphocreatine; PC, phosphocholine; PCA, perchloric acid; PDE, phosphodiesters; Pi, inorganic phosphate; PME, phosphomonoesters; PtdChol, phosphatidylcholine; PtdE, phosphatidylethanolamine; PtdI, phosphatidylinositol; PtdS, phosphatidylserine; SPM, sphingomyelin; UDPS, uridine diphospho-sugar

Key words: carboplatin, cisplatin, cytotoxic drugs, magnetic resonance spectroscopy, ovarian cancer, phospholipid metabolites, paclitaxel

Introduction

Ovarian cancer is the fifth leading cause of death from cancer and the most common cause of death from gynecologic neoplasia in women, due to its detection at advanced stages. Despite significant refinement in treatment options and surgical techniques, the 5-year survival for advanced ovarian cancer still remains low (1,2). In order to improve the outcome of these patients, reliable and accurate diagnostic means are therefore essential. It is well established that the cancerous microenvironment exerts substantial stresses on both cancer and non-cancer cells and often results in a shift in cellular energy production and utilization (3-5). Hence, it seems plausible that investigating the biochemical intermediates and end products within cancerous tissue samples would refine our knowledge of cancer biology.

Magnetic resonance spectroscopy (MRS) is a non-invasive analytical technique which can assess both molecular structural and chemical composition of non-homogeneous biological specimens. This method has provided considerable information on energetic status and cellular metabolism in various tissues and organs particularly in cancer cell cultures and tumorigenic tissues (6,7). In our previous study we applied ^{31}P-MRS to *in vitro* studies of various breast cancer cells grown in culture and observed the effects of drugs on these cells (8). To date, only a few MRS studies have been published on human ovarian pathologies, generally limited to the analysis of fluids aspirated from ovarian cysts (9,10). In the current study,

we sought to determine the metabolic profiles of cells obtained from patients with malignant ovarian tumors and to compare them with non-cancerous cells obtained from patients with benign ovarian cysts using the ^{1}H-MRS method. In addition, we aimed to evaluate the metabolic effects of different anti-mitotic drugs on cells obtained from peritoneal effusions of patients with advanced ovarian cancer using ^{31}P-MRS.

Materials and methods

Patients. Forty-three patients were recruited to this study. Twenty patients had newly diagnosed, histopathologically proven ovarian cancer (study group) and 15 patients had benign ovarian cysts (control group). Characteristics of patients from the study and control groups are presented in Table I. Patient age was not significantly different between the study and control groups (63.2±7.1 vs. 61.3±4.7 years, respectively); however, tumor size was significantly larger in the study group (11.4±3.2 vs. 7.4±2.1 cm, p=0.0001). Most patients in the study group had serous cystadenocarcinoma (80%), either moderately to poorly differentiated (55%) or poorly differentiated (40%) (Table I). Most patients in this group were diagnosed at stage 3 (55%) or 4 (20%). Thirty-five percent of patients had neo-adjuvant chemotherapy prior to surgery. Patients in the control group had either serous (9 patients) or mucinous (4 patients) cystadenoma, or cystadenofibroma (2 patients). All patients underwent explorative laparotomy for tumor resection or debulking in our institution. Tumor size and stage were recorded for all patients during surgery. Tissue samples from ovarian tumor and intra-abdominal metastases (which were present in 15 patients with stage 3-4 disease) or from benign ovarian cysts (in the control group) were excised by the operating physician to an average size of 1 cm^3 and were frozen immediately in liquid nitrogen in a sterile plastic tube. Samples were kept under deep freeze (-80˚C) until analysis. Parallel tissue samples underwent a histopathologic evaluation by a certified pathologist. Another 8 patients (mean age, 62±5 years) with advanced ovarian cancer and cytologically proven cancerous peritoneal effusion were recruited to this study. All patients had received at least one platin- and/or paclitaxel-based treatment cycle (median, 3; range, 1-5) and all underwent a palliative drainage of their peritoneal effusion in our institution. Two hundred milliliters of peritoneal effusion were obtained from each patient for MRS analysis. All subjects signed an informed consent approved by the Institutional Review Board Committee for Human Subjects.

Preparation of samples for MRS analysis. MRS analysis was conducted on both tissue samples and cells obtained from peritoneal effusion. While tissue samples universally required cell extraction before analysis, cells obtained from peritoneal effusions allowed MRS evaluation either in cell extracts or in viable cells embedded in Matrigel (CEM) (see below). The latter option facilitated continuous monitoring of magnetic resonance (MR) spectra following incubation with various anti-mitotic drugs. Cells obtained from peritoneal effusions initially presented a mixture of different cell types. We, therefore, performed several clone separations and sub-cloning in order to create homogenous cultures before MRS analysis. Subsequently, cell cultures were grown in DMEM supplemented with FCS (10%), sodium pyruvate solution 100 mM (1%), L-glutamine solution (200 mM) (1%), MEM vitamin solution (1%), MEM non-essential amino acid solution (1%) and penicillin-streptomycin solution (1%) (Biological Industries, Israel). Cell cultures were grown either in 92x17 mm dishes for further culturing or in 144x21 mm dishes (Nunclon) when larger amounts of cells were required. Cultures were regularly fed every 3-4 days and subcultured by a 1:30 to 1:40 split ratio by detaching cells after one phosphate-buffered saline (PBS) wash with Trypsin (0.05%) EDTA (0.02%) solution (Biological Industries). All cultures were incubated at 37˚C with 10% CO_2.

Preparation of cell extracts from cell cultures and tissue samples. Cells were detached using Trypsin-EDTA solution and collected in a 50-ml tube for centrifugation for 5 min at 1,000 rpm. The supernatant was removed and 1 ml of 0.5 M $HClO_4$ 5 M was added to the tube which was kept over ice during the entire procedure. Incubation in the perchloric acid (PCA) lasted 5 min and the solution was occasionally mixed by vortexing. Frozen tissue samples were washed in liquid nitrogen to assure maximal freezing. Tissues were then crushed into powder and transferred to a 50-ml plastic tube, with PCA (1 M). Tissues were incubated in the acid for 15 min and mixed occasionally. The acid was neutralized to a pH of 7.0 using KOH (5 and 0.5 M). The whole mixture was then centrifuged at 13,000 rpm for 20 min in 4˚C. The supernatant was transferred to a 20-ml plastic bottle and mixed with 0.2-0.4 g Chelex 100 (Bio-Rad, USA) for 1 h at 4˚C, in order to chelate all metals within the solution. The solution was then filtered through a GF/B (1.0-μM pore size) 2.5-cm diameter Glass Microfiber filter (Whatman, UK) into a 150-ml glass flask, and the filtrate was frozen in liquid nitrogen and lyophilized overnight until dried. The dry sample was kept sealed in the flask at -80˚C until MRS analysis.

Preparation of cell extracts before the MRS analysis. The dry extracts were dissolved in 700 μl cold D_2O, mixed and moved to a 1.5 ml Eppendorf tube for 10 min of centrifugation at 10,000 rpm. D_2O enables the lock signal on the MR spectrometer to be used. The solutions were then transferred to a 5-mm MRS tube and kept at 4˚C until analysis. Before MRS analysis for ^{1}H- and ^{31}P-containing compounds, 70 μl of EDTA solution (0.2 M) was added to the MRS tube to remove paramagnetic ions. Samples were constantly kept on ice.

3-Dimensional Matrigel construct. In order to follow changes occurring in living ovarian cancer cells using MRS, the cells were packed in the MRS tube in Matrigel (BD Matrigel™ matrix; BD Biosciences, USA), a solubilized basement membrane preparation extracted from EHS mouse sarcoma (a tumor rich in ECM proteins) whose major components are laminin (56%), followed by collagen IV (31%), heparan sulfate proteoglycans and entactin (8%). Prior to the procedure, Matrigel was thawed at 4˚C in icy water, a flask was filled with 60 ml of fresh medium either with or without drug and a 60-cm long Teflon tube of 0.5 mm i.d. was attached to a sterile 23G needle on a 10 ml syringe. The tube was washed twice with 70% ethanol and the whole apparatus was kept in ethanol until it was used. For each experiment 3 dishes of 144x21 mm

Table I. Patient characteristics.

	Malignant tumor (n=20)	Benign tumor (n=15)
Mean age (years)	63.2±7.1 (n=20)	61.3±4.7 (n=15)
Tumor size (cm)	11.4±3.2	7.4±2.1
Tumor type		
Serous	16 (80%)	9 (60%)
Mucinous	2 (10%)	4 (26.7%)
Clear cell	1 (5%)	0 (0%)
Undifferentiated	1 (5%)	0 (0%)
Other	0 (0%)	2 (13.3%) (cystadenofibroma)
Degree of differentiation		
Well	0 (0%)	N/A
Moderate to poor	11 (55%)	
Poor	8 (40%)	
Undifferentiated	1 (5%)	
Clinical stage		
1	2 (10%)	N/A
2	3 (15%)	
3	11 (55%)	
4	4 (20%)	
Primary	20 (100%)	15 (100%)
Recurrent	0 (0%)	0 (0%)
Previous neo-adjuvant chemotherapy	7 (35%)	N/A

Values are presented as no. (%), means ± SD, or median (range). N/A, not applicable.

were cultured to full confluency. Cells were detached using trypsin and centrifuged for 5 min at 1,000 rpm. The medium was removed and the tube containing the cells was set on ice in a box, which was earlier disinfected with 70% ethanol. Cold (4˚C) Matrigel (1.5 ml) was added to the cells using a cold sterile pipette. The cells and the Matrigel were gently mixed to a homogenous suspension. Matrigel threads were then prepared one after the other as quickly as possible in order to return the cells to the medium rapidly. The suspension was gently drawn into the teflon tube and was left in the tube at room temperature for 30-120 sec until it polymerized. After the whole suspension was transformed into semi-solid threads, the cells were left to incubate in the medium for ~30-33 h in the incubator at 37˚C, in 5% CO_2.

MRS analysis. ^{1}H-MRS and ^{1}H-decoupled ^{31}P-MRS spectra were acquired at 10˚C on a Varian Inova 500 machine which detects ^{1}H nuclei at 500 megaHertz (MHz) and ^{31}P nuclei at 202 MHz. Prior to each series of experiments, the values of T1 and the required 90˚ pulse width were determined and then used for the analysis. MRS experiments of all extracts were carried out using the '5BB' probe at 10˚C and analyzed in 3 ways: First a proton (^{1}H) spectrum was acquired at a spectrometer frequency of 499.791 MHz with a 90˚ pulse, transmitter power of 63 dB and pulse width of 9.1 μsec. The relaxation delay was set to 2.00 sec and the acquisition time lasted 1.892 sec. Sixty-four scans were accumulated to produce the final spectrum. The spectrum from this experiment was then loaded, and the water-suppressed ^{1}H spectrum was detected. The water signal (at 4.65 ppm) from the first detection was chosen and the pre-saturation sequence was activated. Detection parameters included: saturation power of 8 and saturation delay of 3.00 sec. One hundred and twenty-eight scans were accumulated. The spectrometer frequency was then set at 202.319 MHz for the ^{31}P detection. Parameters were set at: transmitter power of 56 dB, pulse width of 7.0 μsec and flip angle of 66.3˚. Broad-band decoupling was activated to suppress the proton detection with a decoupler power of 40 dB without nuclear overhouser enhancement (NOE). Three thousand scans were accumulated to produce the final spectrum. Spectra were manually integrated by marking the beginning and ending of each signal of interest. The first signal marked was automatically set as 1 and was used as a reference. In ^{1}H analysis the signal of adenosine triphosphate (ATP) at 8.25 ppm and in the ^{31}P analysis the signal of β-ATP at -21 ppm were set as references, respectively. All signal integrals were set in tables in MS Excel 2007 sheets. Figures were created using MS Excel 2007.

Anti-mitotic drugs. Three anti-mitotic drugs were used: paclitaxel (Taxol; BMS, USA), cisplatin (Cisplatin; Merck, Vianex, Greece) and carboplatin (Paraplatin; BMS, Italy). Stock concentrations of the drugs were paclitaxel (6 mg/ml), cisplatin (1 mg/ml) and carboplatin (10 mg/ml). Paclitaxel was further diluted in DMSO, and the platinum compounds were diluted in distilled water. In order to determine the effective concentrations of the drugs to be used with the cell cultures, a series of experiments was conducted to determine

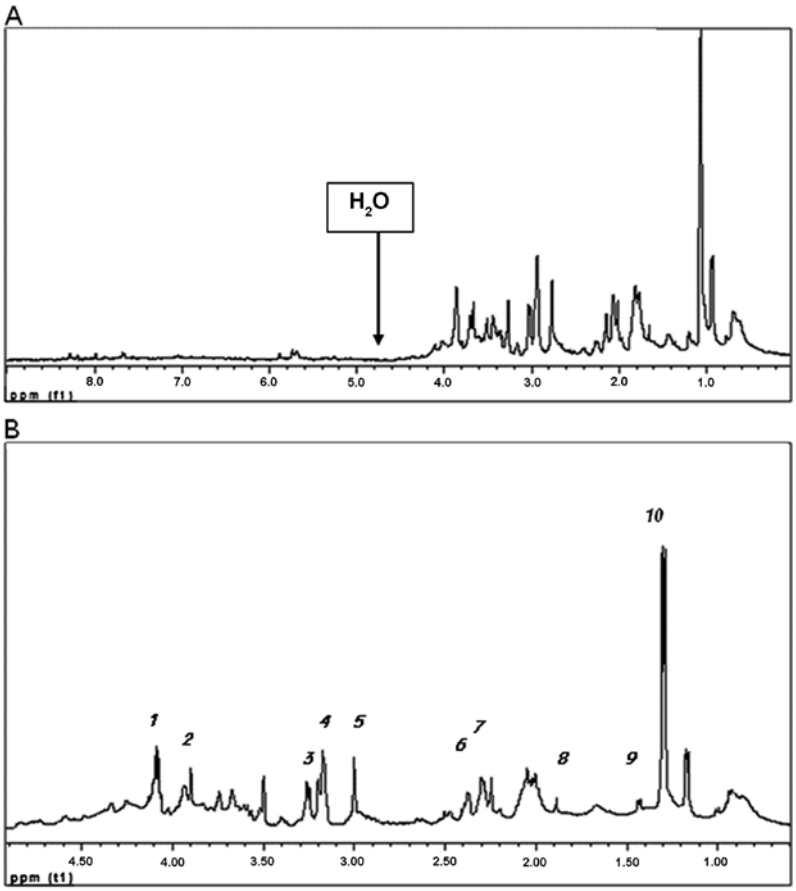

Figure 1. (A) Water-suppressed ^{1}H-NMR spectra of cell extracts from an ovarian tumor. The water signal was suppressed and the smaller signals were consequently more observable. (B) Aliphatic region of the water-suppressed ^{1}H-NMR spectra of tissue sample no. OCR-14-2. Assignments are: 1, lactate CH_2 at 4.12 ppm; 2, creatine + phosphocreatine CH_2 at 3.93-3.95 ppm; 3, taurine N-CH_2 at 3.27 ppm; 4, choline compounds (Chol, PChol, GPC) CH_3 at 3.21-3.24 ppm; 5, creatine + phosphocreatine CH_3 at 3.04-3.05 ppm; 6, glutamine CH_2 at 2.45 ppm; 7, glutamate CH_2 at 2.34 ppm; 8, acetate CH_3 at 1.92 ppm; 9, alanine CH_3 at 1.48 ppm; 10, lactate CH_3 at 1.32 ppm.

LC_{50}. The following procedure was performed at least twice with each cell line. Cells were seeded in a 12-well plate (6 duplicates) at 10,000 cells/ml, 2 ml/well. Approximately 24 h after seeding, the drug was added to 5 of the 6 duplicates in increasing concentrations. Two wells were left untouched, as controls. The middle concentration was close to the estimated LC_{50}; 2 duplicates had higher concentrations and 2 had lower. The volume of the drug solution, which was added to the well, was never higher than 1% of the total volume. After 48 h of incubation with the drugs, the wells were washed with PBS in order to wash away dead cells and the adherent cells were detached using trypsin. Cells were transferred to a cuvette and diluted in PBS to a total volume of 20 ml. They were counted in a Coulter counter, which was calibrated to the proper size of particles after a sample manual counting. Each cuvette was counted 4 times and all counts were compared to the control count of the clean PBS. Counting results were analyzed using MS Excel 2007 and the derived LC_{50} parameters were used in the chemotherapeutic experiments. Cells were incubated with the drugs at LC_{50} for 48 h before MRS analysis.

Statistical analysis. Data are expressed as means ± SD. Statistical significance was assessed by the Student's 2-tailed t-test and analysis of variance as indicated. A P-value <0.05 was considered statistically significant for all comparisons, unless indicated otherwise.

Results

^{1}H-MR spectra of tissue samples. Fig. 1A shows the water-suppressed ^{1}H-MR spectra of a cell extract obtained from an ovarian tumor, using pre-saturation of the water signal. In this study, we chose to concentrate on the signals of the metabolites appearing in the aliphatic region of the spectrum, between 0-5 ppm (Fig. 1B). In order to compare between the different samples in a quantitative manner, a common integration method was used. The integral of ATP at 8.25 ppm was assigned the value of one and all other integrals were calculated relative to it. ^{1}H-MRS revealed a significantly higher intracellular lactate signal at 1.32 ppm (but not at 4.1 ppm) in cells obtained from ovarian tumors as compared to cells obtained from benign ovarian cysts (P=0.005) (Fig. 2A). The total choline compound signal was higher in ovarian cancer cells, however, this difference did not reach statistical significance (P=0.06). No significant differences in ^{1}H-MR spectra between benign and malignant samples were noted in other intracellular compounds (Fig. 2A). After histologic stratification by the degree of differentiation and by primary tumor vs. metastasis, the most prominent MR spectral differences in

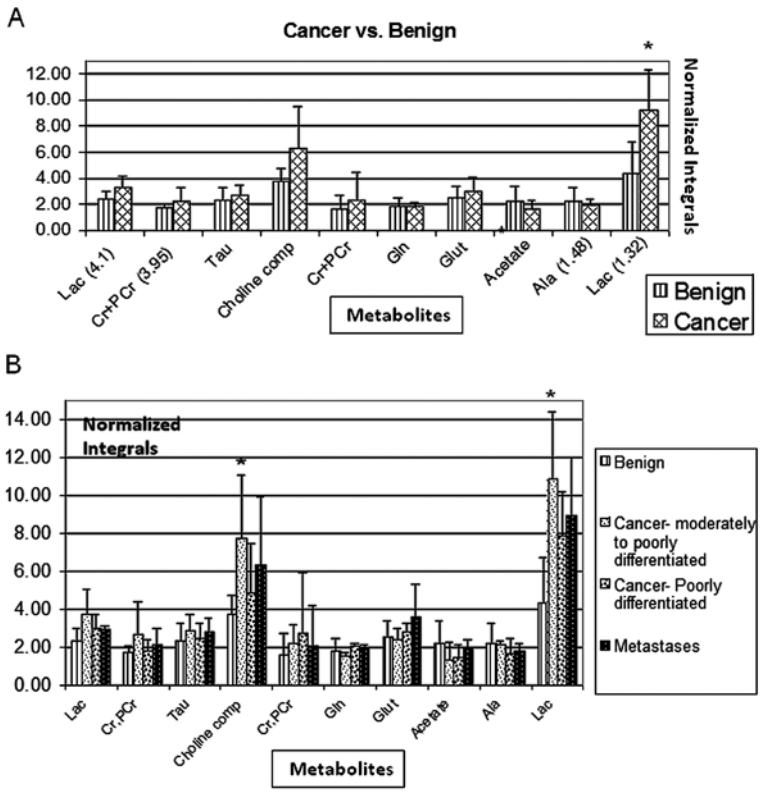

Figure 2. (A) Integrated metabolite signals (normalized to β-ATP) from ^{1}H-MR spectra of cell extracts from benign vs. malignant ovarian tumor samples. Values are presented as means ± SD. Lac, lactate; Cr, creatine; PCr, phosphocreatine; Tau, taurine; Choline comp, total choline compounds; Gln, glutamine; Glut, gluthatione; Ala, alanine. (B) Integrated (normalized to β-ATP) ^{1}H magnetic resonance (MR) spectra of benign vs. malignant samples with stratification by degree of differentiation and by primary tumor vs. metastasis. Values are presented as means ± SD.

Table II. LC_{50} of the anti-mitotic drugs in the cells from peritoneal effusions.

Cell line	Paclitaxel	Cisplatin	Carboplatin
SC1			
Extracted	$5.6x10^{-8}$ M	$5.2x10^{-6}$ M	$2.5x10^{-6}$ M
In Matrigel	$6.1x10^{-7}$ M	$5.1x10^{-5}$ M	$2.4x10^{-5}$ M
SC3			
Extracted	$2.1x10^{-7}$ M	$2.3x10^{-6}$ M	$1.1x10^{-5}$ M
In Matrigel	$2.2x10^{-6}$ M	$2.2x10^{-5}$ M	$1.2x10^{-4}$ M

both lactate (P=0.001) and total choline compounds (P=0.02) between malignant and benign ovarian tumors were noted in the moderately to poorly differentiated histologic subtype (Fig. 2B).

Changes in metabolite levels following chemotherapy. Cells obtained from peritoneal effusions initially presented a mixture of different type of cells. We, therefore, performed several clone separations and subcloning in order to create homogenous cultures adequate for MRS analysis. We eventually isolated 3 purified clones (designated SC1-SC3) which were either grown in monolayer cultures or embedded in Matrigel threads. Cell cultures were incubated with various anti-mitotic drugs at LC_{50} (Table II) and ^{31}P-MRS analysis was performed on either cell extracts [for cells grown in monolayers (CGM)] or on viable cells (for CEM).

The concentration that causes death of 50% of the cells, LC_{50}, was calculated for either CGM or CEM (Table II). The LC_{50} for CEM was higher by one order of magnitude compared to that of cell extracts. After the cultures were incubated with the drugs at the LC_{50} for 48 h, they underwent MRS analysis. In contrast to CGM, CEM allowed continuous monitoring of the changes in ^{31}P-MRS spectra following incubation with cytotoxic drugs. Fig. 3 demonstrates changes in MR spectra of viable SC3 CEM following 48 h of incubation with paclitaxel exhibiting a significant decrease in both phosphodiesters (PDE) and UDPS signals. Fig. 4A exhibits integrated ^{31}P spectra of SC1 cell extracts before and after incubation with either paclitaxel, cisplatin or carboplatin. A significant decrease in GPE, GPC, nicotine adenine diphosphate (NADP) and UDPS was noted in response to all 3 anti-mitotic drugs. Fig. 4B shows ^{31}P-MR spectra of SC3 CEM following incubation with paclitaxel,

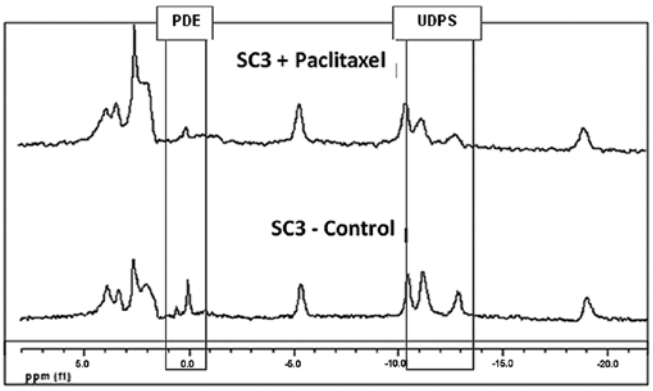

Figure 3. Changes in ^{31}P-MR spectra of viable SC3 cells embedded in Matrigel (CEM) following 44 h of incubation with paclitaxel (Taxol). Significant differences are designated by boxes. PDE, phosphodiesters; UDPS, uridine diphospho-sugar.

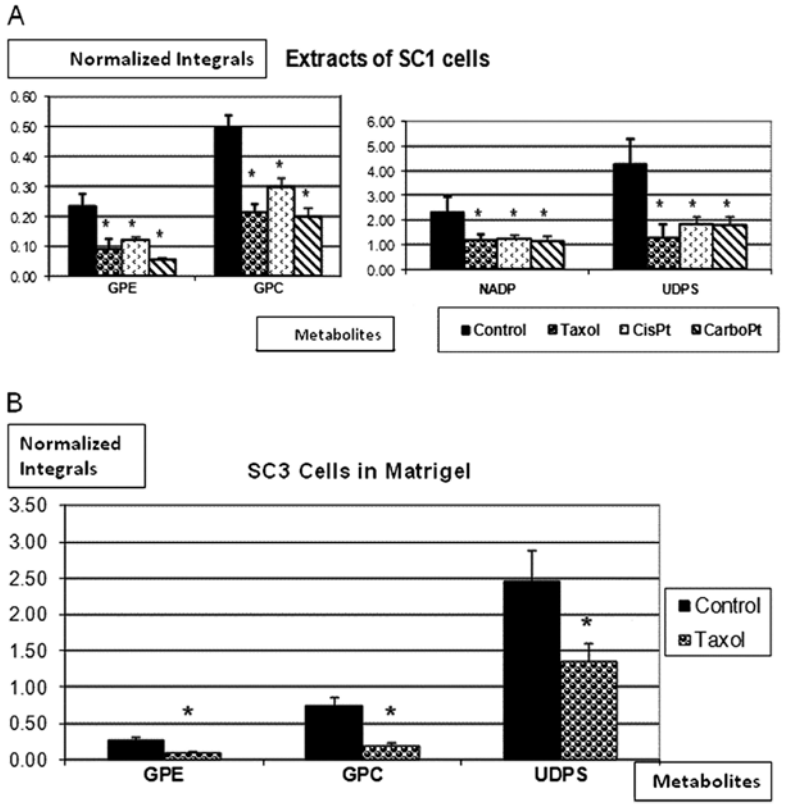

Figure 4. (A) Integrated metabolite signals (normalized to β-ATP) from ^{31}P-MR spectra of SC1 cell extracts before and after cell incubation with paclitaxel (Taxol), cisplatin (CisPt) or carboplatin (CarboPt) for 48 h. Values are presented as means ± SD. *P<0.05 for comparisons between the control and treatment groups. (B) Integrated (normalized to β-ATP) ^{31}P-MR spectra of SC3 cells embedded in Matrigel (CEM) following incubation with paclitaxel. Values are presented as means ± SD. *P<0.05 for comparisons between the control and treatment groups. GPE, glycerophosphoethanolamine; GPC, glycerophosphocholine; UDPS, uridine diphospho-sugar; NADP, nicotine adenine diphosphate.

again exhibiting a significant decrease in GPE, GPC and UDPS signals.

Discussion

In vivo and *ex vivo* MRS is extensively used in biomedical research, particularly for molecular evaluations regarding diagnosis, treatment and prognosis of human malignancies (11-13). The clinical application of MRS to the assessment of breast, brain and prostate cancers has been investigated for several years (14). In contrast, the study of ovarian cancer by MRS has been scant and performed mainly by ^{1}H-MRS. One study managed to discriminate malignant ovarian tumors from normal and benign tissues, based on variations in cellular lipid, lysine/polyamines and creatine/phosphocreatine (PCr) ratios (15). In another study, ^{1}H-MRS of *ex vivo* specimens was utilized to distinguish between normal and malignant ovarian tissues (16). Another study showed that urinary metabolic profiling using MRS managed to detect early-stage breast and ovarian cancers (17). In accordance with these data, the study presented herein, found that *ex vivo* ^{1}H-MRS can identify significant metabolic differences between cells obtained from

ovarian tumors as compared to those originating in benign ovarian cysts.

Increased intracellular concentrations of total Chol-containing compounds have been reported previously in several types of cancer and were suggested to serve as biomarkers for cancer both *in vivo* and *ex vivo* (18,19). Significantly altered proton MRS spectra have been detected in the 3.20 to 3.24 ppm region, typical of trimethylammonium head groups of phosphatidylcholine (PtdChol) precursors and catabolites, such as GPC, free Chol and PC, in malignant transformation of human breast (20-22) and prostate epithelial cells (23). Currently, choline phospholipid metabolism in ovarian tumors has not yet been studied extensively, despite preliminary indications of accumulation of PChol and total Chol in human ovarian tumors and cancer cell lines (16,24-27). In accordance with these data, in the current study, we found higher total choline compound levels in moderately to poorly differentiated (but not in poorly differentiated or metastatic) ovarian tumors as compared to benign ovarian cysts. It should be noted, however, that our ^{1}H-MRS analysis included total Chol levels only and not individual GPC, phosphocholine (PC) or free Chol levels.

Abnormal levels of other tissue metabolites, such as lactate, have also been associated with malignant transformation (28,29). Increased lactate concentrations may be attributed to hypoxia, a common characteristic of solid tumors where lack of oxygen results in glucose being catabolized to lactate. Using *in vitro* ^{1}H-NMR technique for analysis of fluids aspirated from ovarian cysts, Massuger *et al* (9) showed that the amounts of compounds such as lactate, 3-hydroxybutylic acid, pyruvic acid and methionine, were over 6 times higher in malignant as compared to benign cysts. Indeed, in the study presented herein, ^{1}H-MRS revealed significantly higher intracellular lactate levels in malignant vs. benign ovarian tumors. Increased intracellular lactate concentration has been suggested to serve as a biomarker for tumor aggressiveness since high lactate concentration has been correlated with increased risk of radiation resistance, high incidence of distant metastasis and recurrence and low survival rates in several types of cancer (30,31). In our study, lactate levels were most prominently elevated in the moderately to poorly differentiated tumors, a finding which may be attributed to the higher metabolic rate and energy consumption in these cells.

In the current study, we found ^{31}P-MRS to be a useful means for detecting and monitoring metabolic changes in ovarian cancer cells incubated with anti-mitotic drugs. The standard cytotoxic drugs investigated were paclitaxel, an anti-microtubule agent, as well as cisplatin and carboplatin - both alkylating agents. Following incubation with these drugs, a decrease in GPE, GPC, NADP and UDPS levels was observed in the SC1 cell line, obtained from cancerous peritoneal effusions. Furthermore, following incubation with paclitaxel, similar metabolic changes were observed in another (SC3) cell line. These findings are in accordance with a previous study which reported that drug-induced apoptosis causes a decrease in PDE (i.e., GPC and GPE) levels in cancer cells (32), however, they are in contrast with our previous findings in breast cancer cells where a profound elevation in intracellular GPC levels was observed following exposure to antimicrotubule drugs (8). A possible explanation for these contradictive findings is that microtubule dynamics may affect the phospholipid balance differently in different cell types. Alterations in microtubule stability in response to anti-mitotic drugs may change local membrane composition and the interaction of membrane proteins with their lipid environment. Microtubule-disturbing drugs affect the affinity of agonists to their membranal receptors (33), the transmembranal diffusion of phospholipids (34) and PtdChol synthesis (35). GPE and GPC are two of the numerous cytosolic phospholipid metabolites which reflect the condition of the cellular phospholipid system and hence may reflect cytoskeletal stability and dynamics. Both metabolites were found to act as competitive inhibitors of lysophospholipase activity, thus reducing lysophospholipid hydrolysis and downregulating the rate of membrane phospholipid degradation (36).

Acknowledgements

This study was funded by the Zaltzberg Research Fund, Hadassah Medical Organization, Israel.

References

1. National Cancer Institute, http://www.cancer. gov.
2. Jemal A, Siegel R, Ward E, Hao Y, Xu J and Thun MJ: Cancer statistics 2009. CA Cancer J Clin 59: 225-249, 2009.
3. Tennant DA, Durán RV, Boulahbel H and Gottlieb E: Metabolic transformation in cancer. Carcinogenesis 30: 1269-1280, 2009.
4. Vander Heiden MG, Cantley LC and Thompson CB: Understanding the Warburg effect: the metabolic requirements of cell proliferation. Science 324: 1029-1033, 2009.
5. Wise DR, DeBerardinis RJ, Mancuso A, *et al*: Myc regulates a transcriptional program that stimulates mitochondrial glutaminolysis and leads to glutamine addiction. Proc Natl Acad Sci USA 105: 18782-18787, 2008.
6. Zupke C and Foy B: Nuclear magnetic resonance analysis of cell metabolism. Curr Opin Biotechnol 6: 192-197, 1995.
7. Bel JD and Bhakoo KK: Metabolic changes underlying ^{31}P MR spectral alterations in human hepatic tumours. NMR Biomed 11: 354-359, 1998.
8. Sterin M, Cohen JS, Mardor Y, Berman E and Ringel I: Levels of phospholipid metabolites in breast cancer cells treated with antimitotic drugs: a ^{31}P-magnetic resonance spectroscopy study. Cancer Res 61: 7536-7543, 2001.
9. Massuger LF, van Vierzen PBJ, Engelke U, Heerschap A and Wevers RA: ^{1}H-magnetic resonance spectroscopy: a new technique to discriminate benign from malignant ovarian tumors. Cancer 82: 1726-1730, 1998.
10. Boss EA, Moolenaar SH, Massuger LFAG, Boonstra H, Engelke UFH, de Jong JGN and Wevers RA: High-resolution proton nuclear magnetic resonance spectroscopy of ovarian cyst fluid. NMR Biomed 13: 297-305, 2000.
11. Podo F: Tumour phospholipid metabolism. NMR Biomed 12: 413-439, 1999.
12. Tosi R and Tugnoli V (eds): Nuclear Magnetic Resonance Spectroscopy in the Study of Neoplastic Tissue. Nova Science Publishers, Inc., New York, NY, pp1-444, 2005.
13. Gillies RJ and Morse DL: In vivo magnetic resonance spectroscopy in cancer. Annu Rev Biomed Eng 7: 287-326, 2005.
14. Kwock L, Smith JK, Castillo M, *et al*: Clinical role of proton magnetic resonance spectroscopy in oncology: brain, breast, and prostate cancer. Lancet Oncol 7: 859-868, 2006.
15. Mackinnon WB, Russell P, May GL and Mountford CE: Characterization of human ovarian epithelial tumors (ex vivo) by proton magnetic resonance spectroscopy. Int J Gynecol Cancer 5: 211-221, 1995.
16. Wallace JC, Raaphorst GP, Somorjai RL, *et al*: Classification of ^{1}H MR spectra of biopsies from untreated and recurrent ovarian cancer using linear discriminant analysis. Magn Reson Med 38: 569-576, 1997.
17. Slupsky CM, Steed H, Wells TH, *et al*: Urine metabolite analysis offers potential early diagnosis of ovarian and breast cancers. Clin Cancer Res 16: 5835-5841, 2010.

18. Podo F, Canevari S, Canese R, Pisanu ME, Ricci A and Iorio E: MR evaluation of response to targeted treatment in cancer cells. NMR Biomed 24: 648-672, 2011.
19. Katz-Brull R, Lavin PT and Lenkinski RE Clinical utility of proton magnetic resonance spectroscopy in characterizing breast lesions. J Natl Cancer Inst 94: 1197-1203, 2002.
20. Aboagye EO and Bhujwalla ZM: Malignant transformation alters membrane choline phospholipid metabolism of human mammary epithelial cells. Cancer Res 59: 80-84, 1999.
21. Glunde K, Jie C and Bhujwalla M: Molecular causes of the aberrant choline phospholipid metabolism in breast cancer. Cancer Res 64: 4270-4276, 2004.
22. Glunde K, Ackerstaff E, Natarajan K, Artemov D and Bhujwalla ZM: Real-time changes in ^{1}H and ^{31}P NMR spectra of malignant human mammary epithelial cells during treatment with the anti-inflammatory agent indomethacin. Magn Reson Med 48: 819-825, 2002.
23. Ackerstaff E, Pflug BR, Nelson JB and Bhujwalla ZM: Detection of increased choline compounds with proton nuclear magnetic resonance spectroscopy subsequent to malignant transformation of human prostatic epithelial cells. Cancer Res 61: 3599-3603, 2001.
24. Iorio E, Mezzanzanica D, Alberti P, *et al*: Alterations of choline phospholipid metabolism in ovarian tumor progression. Cancer Res 65: 9369-9376, 2005.
25. Canese R, PIsanu ME, Mezzanzanica D, *et al*: Characterisation of in vivo ovarian cancer models by quantitative ^{1}H magnetic resonance spectroscopy and diffusion-weighted imaging. NMR Biomed 25: 632-642, 2012.
26. Esseridou A, Di Leo G, Sconfienza LM, *et al*: In vivo detection of choline in ovarian tumors using 3D magnetic resonance spectroscopy. Invest Radiol 46: 377-382, 2011.
27. Iorio E, Ricci A, Bagnoli M, Pisanu ME, *et al*: Activation of phosphtidylcholine cycle enzymes in human epithelial ovarian cancer cells. Cancer Res 70: 2126-2135, 2010.
28. Cheng LL, Chang IW, Smith BL and Gonzalez RG: Evaluating human breast ductal carcinomas with high-resolution magic-angle spinning proton magnetic resonance spectroscopy. J Magn Reson 135: 194-202, 1998.
29. Tessem MB, Swanson MG, Keshari KR, *et al*: Evaluation of lactate and alanine as metabolic biomarkers of prostate cancer using ^{1}H HR-MAS spectroscopy of biopsy tissues. Magn Reson Med 60: 510-516, 2008.
30. Brizel DM, Schroeder T, Scher RL, Walenta S, Clough RW, Dewhirst MW and Mueller-Klieser W: Elevated tumor lactate concentrations predict for an increased risk of metastases in head-and-neck cancer. Int J Radiat Oncol Biol Phys 51: 349-353, 2001.
31. Walenta S, Wetterling M, Lehrke M, Schwickert G, Sundfor K, Rofstad EK and Mueller-Klieser W: High lactate levels predict likelihood of metastases, tumor recurrence, and restricted patient survival in human cervical cancers. Cancer Res 60: 916-921, 2000.
32. Huang Z, Tong Y, Wang J and Huang Y: NMR studies of the relationship between the changes of membrane lipids and the cisplatin resistance of A549/DDP cells. Cancer Cell Int 3: 5, 2003.
33. Hanauske AR, Depenbrock H, Shirvani D and Rastetter J: Effects of the microtubule-disturbing agents docetaxel (Taxotere), vinblastine and vincristine on epidermal growth factor-receptor binding of human breast cancer cell lines in vitro. Eur J Cancer 30A: 1688-1694, 1994.
34. Chahine JMEH, Cribier S and Devaux PF: Phospholipid transmembrane domains and lateral diffusion in fibroblasts. Proc Natl Acad Sci USA 90: 447-451, 1993.
35. Pike MC, Kredich NM and Snyderman R: Influence of cytoskeletal assembly on phosphatidylcholine synthesis in intact phagocytic cells. Cell 20: 373-379, 1980.
36. Fallbrook A, Turenne SD, Mamalias N, Kish SJ and Ross BM: Phosphatidylcholine and phosphatidylethanolamine metabolites may regulate brain phospholipid catabolism via inhibition of lysophospholipase activity. Brain Res 834: 207-210, 1999.